Integrated Thermal Modulation and Deflection of Viscous Microjets with Applications to Continuous Inkjet Printing

E. P. Furlani[1], A. G. Lopez[1], K. C. Ng[1], and C. Anagnostopoulos[2]

[1]Eastman Kodak Research Laboratories
1999 Lake Avenue, Rochester, New York 14650-2216
edward.furlani@kodak.com

[2]Department of Mechanical Engineering and Applied Mechanics
University of Rhode Island
Kingston RI 02881

ABSTRACT

We present a novel CMOS/MEMS microfluidic device that enables the controlled production and redirection of streams of picoliter-sized droplets at frequency rates in the hundreds of kilohertz range. Droplet generation and jet manipulation are achieved using voltage-controlled thermal modulation, at modest temperatures and with no moving elements. We discuss the fabrication and operating physics of the device and we compare experimental performance data with 3D CFD simulations. We discuss applications of this device to continuous inkjet printing.

Keywords: micro-drop generator, thermal jet deflection, thermo-capillary instability, continuous inkjet printing, Marangoni instability

1 INTRODUCTION

Microfluidic devices are finding increasing use in a broad range of applications that involve the production and controlled delivery of micro-droplets. The most notable and commercially successful of these is inkjet printing wherein streams of picoliter-sized drops are ejected at high repetition rates onto a media to render an image. Inkjet printing can be broadly divided into two distinct printing methods; drop-on-demand (DOD) printing and continuous inkjet printing (CIJ). In DOD printing, droplets are produced as needed to form the image. In CIJ printing, droplets are produced continuously but only a fraction of these are used to form the image. The unused droplets are deflected and guttered prior to reaching the image, and this unused ink is recycled to the printhead. In this presentation we discuss a novel CMOS/MEMS microfluidic device that enables the controlled production and redirection of streams of picoliter-sized droplets at frequency rates in the hundreds of kilohertz range [1-4]. This device it well suited for CIJ printing as well as numerous other applications.

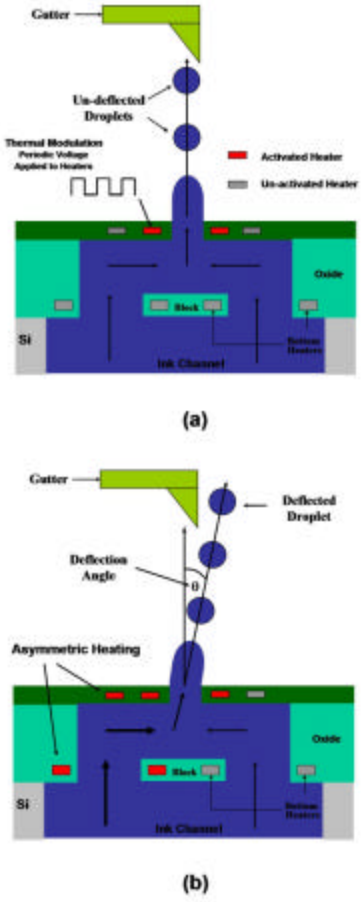

Figure 1: Integrated thermal modulation and deflection of a microjet: (a) symmetric modulation of heaters near the orifice produces a straight stream of droplets, which are recirculated; (b) asymmetric modulation of heaters near the orifice and in the blocking structure produces a deflected stream of droplets.

NSTI-Nanotech 2008, www.nsti.org, ISBN 978-1-4200-8505-1 Vol. 3

2 DEVICE PHYSICS

Our microfluidic device consists of a pressurized reservoir that feeds a micro-nozzle manifold with hundreds of active orifices, each of which produces a continuous jet of fluid. An integrated cylindrical blocking structure is suspended beneath each orifice (Figs. 1 and 2a). This structure splits the flow from the reservoir into two

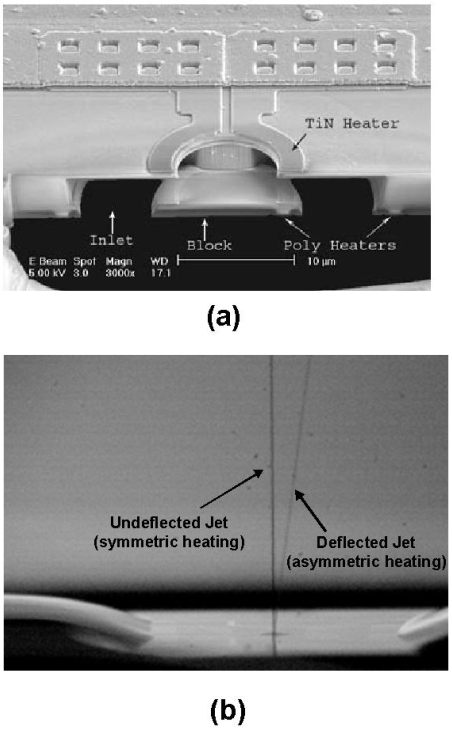

Figure 2: Experimental characterization: (a) fabricated MEMS/CMOS nozzle structure; (b) two adjacent jets (aligned into the page), the front jet is symmetrically modulated producing a straight stream of droplets, the second jet is asymmetrically modulated producing a deflected stream of droplets.

opposing flows that merge immediately beneath the orifice to form the jet. Droplet generation and jet deflection are achieved using voltage-controlled thermal modulation of the fluid. This is achieved using individually addressable resistive heater elements that are integrated into the nozzle plate around each orifice, and also into the suspended blocking structure as shown in Figs 1 and 2a. The heaters are configured to enable symmetric or asymmetric heating. Modulated symmetric heating produces a straight stream of droplets whereas asymmetric heating causes the stream to deflect (Fig. 1).

To modulate a jet, a periodic voltage is selectively applied to the embedded heaters, which causes a periodic diffusion of thermal energy from the heaters into the fluid. Thus, the temperature of fluid, and hence the temperature dependent fluid properties, especially viscosity and surface tension, are modulated near the orifice. This thermal modulation causes two distinct effects; droplet generation and jet deflection.

Droplet production is primarily caused by the modulation of surface tension at the orifice [5-8]. It is well known that slender jets of fluid are inherently unstable and breakup into droplets when subjected to the slightest perturbation. Periodic heating near the orifice produces a modulation of surface tension σ, which produces the perturbation. Specifically, to first order, the temperature dependence of σ is given by $\sigma(T) = \sigma_0 - b(T - T_0)$, where $\sigma(T)$ and σ_0 are the surface tension at temperatures T and T_0, respectively. The pulsed heating near the orifice modulates σ at a wavelength $\lambda = v_0\tau$, where v_0 is the jet velocity and τ is the period of the heat pulse. The down-stream advection of thermal energy gives rise to a spatial variation (gradient) of surface tension along the jet. This produces a shear stress at the free-surface, which is balanced by inertial forces in the fluid, thereby inducing a Marangoni flow towards regions higher surface tension (from warmer regions towards cooler regions). This causes a deformation of the free-surface (slight necking in the warmer regions and ballooning in the cooler regions) that ultimately leads to instability and drop formation [7-8]. The drop volume can be adjusted on demand by varying τ, i.e., $V_{drop} = \pi r_0^2 v_o \tau$, where r_0 is the jet radius. Thus, longer pulses produce larger drops, shorter pulses produce smaller drops, and different sized drops can be produced from each orifice as desired.

Jet deflection is primarily caused by the asymmetric heating of the blocking structure as shown in Fig. 2b. This causes a modulation of viscosity, which results in an increase in the fluid velocity near the activated heater. Thus, there is an imbalance in fluid momentum in the opposing flows that form the jet. This imbalance is carried by the jet through the nozzle resulting in a deflection of the jet away from the heated side as it leaves the orifice. The jet can be deflected from one side of the orifice to the opposite side as needed by applying voltage to the appropriate heaters on either side of the blocking structure. Modulated symmetric heating produces a straight stream of droplets whereas asymmetric heating causes the stream to deflect. The ability to redirect the jet/droplets is useful for applications such as continuous inkjet printing where only a fraction of the generated droplets are used to render an image, and the unused droplets are guttered and recirculated to the reservoir. The integrated CMOS-based thermal modulation and deflection capability of our device represents distinct advantages over conventional continuous inkjet printing systems that rely on piezoelectric driven drop generation and electrostatic deflection of charged droplets.

3 DEVICE FABRICATION

Micro-nozzles with a recessed blocking structure and embedded heaters as shown in Fig. 2a were fabricated using silicon VLSI technology and MEMS fabrication techniques. Arrays of such nozzles were fabricated on standard CMOS wafers containing the logic and drive circuits are in process. Following is the fabrication sequence for lateral flow nozzles on wafers that have not gone through a CMOS process.

(Steps 1-12 would normally be part of the CMOS process)

1) Grow thermal oxide 4000 A.
2) Low-pressure chemical vapor deposition (LPVCD) doped polysilicon 4000A.
3) Define bottom heaters. Dry etch 4000A Poly using chlorine chemistry.
4) Thermal oxidation of polysilicon heater (500 A oxide).
5) Deposit LPCVD TEOS ($Si(OC_2H_5)_4$) 2000A.
6) Deposit LPCVD borophosphosilicate glass (BPSG) 5000A.
7) Define and open contacts to Poly heaters.
8) Sputter TiW/Al (2000A/6000A) for electrical interconnect.
9) Define and dry etch TiW/Al using chlorine chemistry.
10) Deposit 5 µm PECVD oxide.
11) Chemical mechanical polishing (CMP) of oxide (remove approximately 1 µm).
12) Define fluid inlets and partially dry etch oxide, 1.5 µm.

(Steps 13-30 MEMS portion of the process)

13) Define blocks and dry etch remaining oxide, 3.5 µm, to reach the Silicon surface at the inlets.
14) Coat, expose, develop, and bake 10 ∝m polyimide.
Polyimide HD8000 by HD Microsystems
15) CMP polyimide using Cabot W-A400 slurry (Al_2O_3).

- Tool by Strausbaugh model 6EC Planarizer.
- Two steps: Removal rate: 5.5 ∝m/minute and 0.5 ∝m/minute.

16) Megasonic bath clean to remove CMP slurry. H_2O: H_2O_2: NH_4OH 40:2:1
17) Deposit bottom passivation layers PECVD TEOS/ Nitride/ TEOS (2500A/ 2000A/ 2500A).
18) Sputter Ti/TiN (50A/600A) as top heater material.
19) Define and dry etch Ti/TiN top heaters using fluorine chemistry.
20) Deposit PECVD TEOS/Nitride (1500A/1500A).
21) Define and open contacts to TiN heaters.
22) Sputter Al (6000A) for electrical interconnect.
23) Define and dry etch Al using chlorine chemistry.
24) Deposit 3000A PECVD Nitride top passivation layer.
25) Define and etch nozzle bore by dry etching Nitride/ Oxide/ Oxide/ Nitride/ Oxide stack (4500A/ 1500A/ 2500A/ 2000A/ 2500A).
26) Define and open contact to bond pads by dry etching dielectric stack.
27) Thin wafer down to 300 µm.

- Tool by Strausbaugh model 7AA-II
- Removal rate: 150 ∝m/minute.

28) Define fluid channels in the backsides of wafers.
29) Etch through wafer with STS tool using Bosch process.
30) Remove sacrificial polyimide using oxygen chemistry.

4 DEVICE CHARACTERIZATION

We characterized fabricated devices to determine the jet deflection as a function of heater power and drive frequency. All measurements were made using water. We first measured static jet deflection as a function of heater power for two different heating modes. In the first mode, an incrementally increasing voltage was applied to the heater on the left side of the orifice, and the steady state jet deflection was measured at each voltage level. In the second mode, the same procedure was applied using the heater on the left side of the blocking structure. In both cases we found that deflection increased with applied power (Fig.3). Furthermore, for a given power, a larger deflection was achieved using the heater in the blocking structure. The reason for this is because this heater creates a more effective imbalance of fluid momentum than the orifice heater.

We also measured the jet deflection as a function of drive frequency. To do so, we applied an alternating voltage to left and right side heaters in both the orifice and

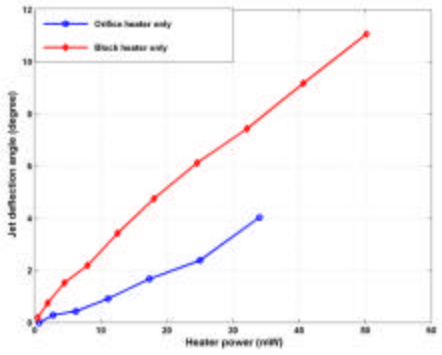

Figure 3: Jet deflection vs. heater power.

the blocking structure. The voltage was synchronized so that the left side heating was 180° out of phase with respect to the right side heating. The periodic alternating heating caused the jet to oscillate back and forth and simultaneously create droplets downstream. The deflection angle vs. drive

frequency along with a strobbed picture of the deflected streams of droplets that evolve from the oscillating jet are shown in Fig. 4. The deflection angle decreases with frequency because of the thermal time constant required for an activated heater to cool to ambient temperature. Note

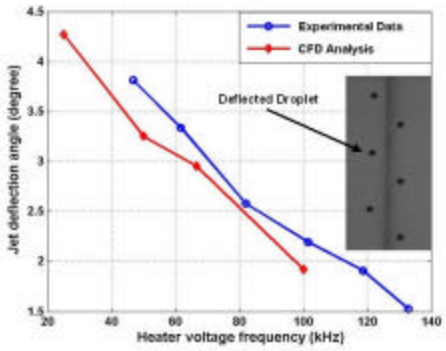

Figure 4: Jet deflection vs. frequency (experimental data and CFD analysis); strobbed image of deflected streams of droplets.

that a working deflection of 1.5 degrees is obtained at a frequency of 132 kHz.

5 DEVICE MODELING

We modeled the performance of the device using 3D CFD. The FLOW-3D software was used for the analysis. The 3D CFD computational domain is shown in Figure 5. The jet deflection angle is predicted by computing the center of mass of the fluid in a control volume near the top of the jet. The predicted deflection vs. frequency data is compared to with corresponding experimental data in Fig. 4. The CFD analysis tended to under predict the measured deflection data. We attribute this to the limited size of the computational domain and the imposition of boundary conditions that did not fully reflect the effects of the neglected physical domain.

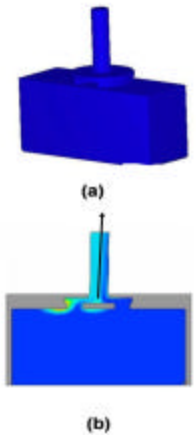

Figure 5: 3D CFD analysis: (a) perspective of internal fluid flow; (b) temperature distribution in the fluid and jet deflection due to asymmetric left-sided heating.

6 CONTINUOUS INKJET PRINTING

A CIJ printhead consists of arrays of orifices wherein each orifice produces a continuous stream of droplets. Only a fraction of the droplets are used to form the image; unused droplets are deflected, guttered and recycled. In a conventional CIJ system, droplet generation is achieved using a piezoelectric transducer, and deflection is achieved using an electrostatic field and charged droplets. The device presented above has distinct advantages in this regard as it enables both droplet production and deflection in an integrated package, thereby eliminating the need for the piezoelectric and electrostatic components altogether. The device has additional advantages in that it enables system miniaturization, higher print resolution, lower production costs, and higher reliability as compared to conventional CIJ systems.

REFERENCES

[1] C. N. Anagnostopoulos, J. M. Chwalek, C. N. Delametter, G. A. Hawkins, D. L. Jeanmaire, J. A. Lebens, A. Lopez and D. P. Trauernicht, "Micro-jet nozzle array for precise droplet and steering having increased droplet deflection," Proc. Transducers 03 Conf. P 368-371, 2003.

[2] J. M. Chwalek, D. P. Trauernicht, C. N. Delametter, R. Sharma, D. L. Jeanmaire, C. N. Anagnostopoulos, G. A. Hawkins, B. Ambravaneswaran, J. C. Panditaratne, and O. A. Basaran, "A new method for deflecting liquid microjets," Phys. of Fluids **14**, 6, 37-40, 2002.

[3] D.P. Trauernicht, C.N. De lametter, J.M. Chwalek, D.L. Jeanmaire, and C.N. Anagnostopoulos, "Performance of Fluids in Silicon-Based Continuous Inkjet Printhead Using Asymmetric Heating," Proc. IS&T NIP17: Int. Conf. on Digital Printing Technologies, pp. 295-298, 2001.

[4] C.N. Delametter, J.M. Chwalek, and D.P. Trauernicht, "Deflection Enhancement for Continuous Ink Jet printers," U.S.Patent 6,497,510, Issued Dec. 24, 2002

[5] E. P. Furlani, "Temporal instability of viscous liquid microjets with spatially varying surface tension," J. Phys. A: Math. and Gen. **38**, 263-276, 2005.

[6] E. P. Furlani, "Thermal Modulation and Instability of Viscous Microjets", proc. NSTI Nanotechnology Conference 2005.

[7] E. P. Furlani, B. G. Price, G. Hawkins, and A. G. Lopez, "Thermally Induced Marangoni Instability of Liquid Microjets with Application to Continuous Inkjet Printing", Proc. NSTI Nanotechnology Conference, 2006.

[8] E. P. Furlani and K. C. Ng, "Numerical Analysis of Nonlinear Deformation and Breakup of Slender Microjets with Application to Continuous Inkjet Printing", Proc. NSTI Nanotechnology Conference, 2007.